

# A Design of Experiments Approach to Analyze the Effects of Hydroxyapatite and Maleic Anhydride Grafted Polyethylene Contents on Mechanical, Thermal and Biocompatibility Properties of Green High-Density Polyethylene-Based Composites

Mário Augusto Morozo<sup>a,b</sup> , Glaucea Warmeling Duarte<sup>c</sup> , Luciano Luiz Silva<sup>d</sup> ,

Josiane Maria Muneron de Mello<sup>d,e</sup> , Micheli Zanetti<sup>d</sup>, Gustavo Lopes Colpani<sup>d,e</sup> ,

Márcio Antônio Fiori<sup>d,e,f</sup>, Leonardo Bresciani Canto<sup>a,g\*</sup> 

<sup>a</sup>Universidade Federal de São Carlos, Programa de Pós-Graduação em Ciência e Engenharia de Materiais, São Carlos, SP, Brasil.

<sup>b</sup>Universidade Comunitária da Região de Chapecó, Escola Politécnica, Chapecó, SC, Brasil.

<sup>c</sup>Centro universitário em Santa Catarina, Núcleo de Pesquisa e Extensão em Engenharia e Tecnologia, Orleans, SC, Brasil.

<sup>d</sup>Universidade Comunitária da Região de Chapecó, Programa de Pós-Graduação em Ciências Ambientais, Chapecó, SC, Brasil.

<sup>e</sup>Universidade Comunitária da Região de Chapecó, Pós de Liderança em Tecnologia, Chapecó, SC, Brasil.

<sup>f</sup>Universidade Tecnológica Federal do Paraná, Departamento de Física, Pato Branco, PR, Brasil.

<sup>g</sup>Universidade Federal de São Carlos, Departamento de Engenharia de Materiais, São Carlos, SP, Brasil.

Received: December 14, 2022; Revised: March 23, 2023; Accepted: April 14, 2023

Composites based on green high-density polyethylene (G-HDPE) and hydroxyapatite (HA) compatibilized with maleic anhydride grafted high-density polyethylene (HDPE-g-MAH) were developed in this work. The main objective was to evaluate the effects of HA and HDPE-g-MAH contents on the mechanical and thermal properties and hydrolytic degradation of composites through design of experiments and statistical analysis, as well as to evaluate the hemolytic stability. Hydroxyapatite acts as a reinforcing agent for the G-HDPE matrix while the HDPE-g-MAH acts as a compatibilizing agent, improving the dispersion of the HA particles in the polymer matrix and thus increasing the mechanical properties. The crystallization temperature and the degree of crystallinity of the polymer matrix were increased with the addition of HA, suggesting the filler acts as a heterogeneous nucleating agent. Hemolysis tests performed on a composite sample with best mechanical performance did not indicate significant hydrolytic degradation, which suggests this composite is a promising material to be used in bone tissue engineering, for application in implants and bone grafts.

**Keywords:** Green Polymers, Green Polyethylene, Hydroxyapatite, Green Polymer Hydroxyapatite Composites, Green HDPE and hydroxyapatite composites, HDPE-g-MAH, Design of experiments.

## 1. Introduction

Composites based on polyethylene (PE) filled with hydroxyapatite (HA) have been widely studied for bone tissue engineering applications, mainly in implants and grafts, as they can mimic the properties of natural bones<sup>1-7</sup>. PE is generally preferred as a matrix in these composites due to its chemical stability, good mechanical properties and biocompatibility. Other hydroxyapatite-based polymer composites have been also developed for biomedical applications, mostly in scaffolds<sup>8,9</sup>.

Hydroxyapatite (HA) is a polar compound of calcium phosphate ( $\text{Ca}_{10}(\text{PO}_4)_6(\text{OH})_2$ ) and its atoms are spatially organized in hexagonal structures<sup>10</sup>. HA is widely accepted as a biocompatible material due to its osteogenic property and ability to form strong bonds with bone tissues<sup>3,11</sup>. Due to structural, chemical and mechanical similarities with

the bones and teeth of humans and animals, hydroxyapatite is widely used as a base and coating for orthopedic and dental implants<sup>12,13</sup>.

The studies on PE/HA composites reported in the literature have been used a petroleum-derived polymer<sup>1-7</sup>. Nevertheless, the use of new materials and processes to develop composite materials with innovative properties or with mitigation of environmental impacts is a worldwide trend. Thereby, replacement of the traditional polymers, synthesized from chemical and petrochemical processes, by polymers synthesized from green chemical and green processes is a strong tendency<sup>14,15</sup>. Green polymers have been a recent opportunity to develop a new class of polymeric composites with environmental responsibility and without compromising their properties in relation to traditional composites.

\*e-mail: leonardo@ufscar.br

Green polymerization principles are one of the worldwide strategies to reduce the consumption of hazardous materials in chemical applications and have been used to synthesize, for example, polymeric membranes<sup>16</sup>, polymers for electrical applications<sup>17</sup> and green high-density polyethylene (HDPE) reinforced with basalt fiber and agricultural fillers<sup>18</sup>. The basis for synthesizing green polyethylene is green ethylene. Green ethylene has been synthesized from ethanol dehydration reactions carried out at high temperatures and with specific solid catalysts<sup>19</sup>. This concept has enabled the synthesis of high-density polyethylene (HDPE), which can be considered a bio-based plastic (bioplastics) and can potentially contribute to improving the environmental performance of future plastic products<sup>20</sup>.

Maleic anhydride grafted high density polyethylene (HDPE-g-MAH) has been shown to be a good interfacial compatibilizer agent for HDPE/HA composites<sup>21,22</sup>. This is due to chemical interactions between the maleic anhydride unit and hydroxyapatite polar groups, which produce a strong interface during melting processing that helps to disperse HA into HDPE matrix. Moreover, maleated PE has been successfully used as a compatibilizer agent for other PE based composites<sup>23,24</sup>.

Although the studies on PE/HA composites uncompatibilized and compatibilized with maleated polyethylene reported in the literature have brought insights into the effects of composition on the mechanical performance, a statistical analysis approach is still lacking.

In this study, composites based on green high-density polyethylene (G-HDPE) as the polymer matrix, hydroxyapatite (HA) as the calcium phosphate phase and maleic anhydride grafted polyethylene (HDPE-g-MAH) as a compatibilizing agent were developed. The main objective was to evaluate the effects of hydroxyapatite and compatibilizer contents on the mechanical and thermal properties and hydrolytic degradation stability of the composites through design of experiments (DOE), analysis of variance (ANOVA) and Tuckey test. The composition that provided the best mechanical performance was then subjected to hemolysis test. From the analysis of the mechanical properties obtained by tensile, flexural and impact tests, as well as thermal analysis (DSC) and biological tests (hydrolytic degradation and hemolysis), it was possible to obtain a polymer composite with potential application in biological devices.

## 2. Materials and Methods

### 2.1. Materials

Green high-density polyethylene (G-HDPE) is a biobased grade (SGE 7252) supplied by Braskem company, Brazil. The G-HDPE has a melt flow rate (MFR) of 2 g 10 min<sup>-1</sup> (ASTM D1238: 190 °C/2.16 kg) and a density of 0.952 g cm<sup>-3</sup> (ASTM D792). Although this grade is not specific to biomedical applications, it served as a proof of concept for the effects of composite composition on the studied properties. The HDPE-g-MAH is a high-density polyethylene modified with maleic anhydride (0.8% to 1.2%) grade (Polybond 3009) supplied by Addivant TM company. The HDPE-g-MAH has a melt flow rate (MFR) of 5 g 10 min<sup>-1</sup> (ASTM D1238: 190 °C/2.16 kg) and a density of 0.950 g cm<sup>-3</sup> (ASTM D792).

The HDPE and HDPE-g-MAH were cryogenically grounded in a CF Bantam Micron Powder Systems mill and then dried for 12 h (overnight) in an oven with air circulation at 45 °C.

Hydroxyapatite (HA) was synthesized by the method of precipitation in an aqueous medium<sup>4</sup>, using calcium oxide (CaO, 95%, Dinâmica Química Contemporânea Ltda) and phosphoric acid (H<sub>3</sub>PO<sub>4</sub>, 85%, Dinâmica Química Contemporânea Ltda). The Ammonium hydroxide (NH<sub>3</sub>OH, 28 – 30%, Química Moderna Indústria e Comércio Ltda) was used as a pH regulator. The precipitate was separated from suspension by filtration using a filter paper (Whatman n°1) and vacuum pump and then placed in an oven for 24 hours at 100°C for drying. After drying, the sample was cooled in a desiccator until it reached room temperature and then it was grounded using a mortar and agate pestle until it became a powder. The dried powder was calcined in a muffle furnace (Logen Scientific, LSSX2-4-10NP) with a heating rate of 8 °C min<sup>-1</sup> until 800 °C. The residence time in the oven in this heating interval was 2 h.

### 2.2. Characterization of the hydroxyapatite (HA)

The hydroxyapatite was characterized by X-Ray Diffraction (XRD) in a diffractometer (Bruker D8 Advance Eco) with copper source ( $\lambda = 1,54$  nm) and in a range of 2Theta from 5° to 80°, with a step time of 0.226 seconds and a diffraction slit of 0.6 mm. The quantification of crystalline phases and crystallite size were performed using the Rietveld and Scherrer methods, respectively.

The chemical composition of the hydroxyapatite was confirmed by X-ray Fluorescence Spectroscopy (Panalytical, Axios Max) and the granulometric studies were performed with a Laser Particle Size Analyzer (Laser Diffraction - Cilas, model 1064).

The morphology of the hydroxyapatite (HA) was assessed by SEM using a FEI MAGELLAN 400 L instrument. A sample of HA was dispersed in ethyl alcohol (2 vol%) with ultrasound, dripped onto a thin aluminum sheet and then sputter coated with gold prior to SEM examination.

### 2.3. Experimental approach

The G-HDPE/HA/HDPE-g-MAH compositions were defined using a design of experiments method of central composition with two factors (variables) and three central points. The hydroxyapatite (HA) and maleic anhydride grafted polyethylene (HDPE-g-MAH) contents were defined as independent variables, with 5.9 wt% and 34.1 wt% being the minimum and maximum values. The HA content was relative to the total weight of the composite and the HDPE-g-MAH content was relative to the weight of the hydroxyapatite (HA) in the composite. Thus, according to the design of experiments, eleven formulations were established for the G-HDPE/HA/HDPE-g-MAH composites (Table 1). Neat G-HDPE and G-HDPE/HA (10, 20 and 30 wt% HA) samples with no compatibilizer were also prepared for comparison.

### 2.4. Melt processing of the G-HDPE/HA/HDPE-g-MAH composites

G-HDPE, G-HDPE/HA and G-HDPE/HA/HDPE-g-MAH samples were prepared in an APV Baker Perkins Equipments

and Systems (model MP-19TC) intermeshing co-rotating twin-screw extruder (Co-TSE) with a screw diameter (D) of 19 mm and length to diameter ratio (L/D) of 25:1. The screw configuration used is comprised of two sets of staggered kneading paddles in between conveying elements. The set upstream contains fourteen forward kneading paddles at staggered angles of 30°, 60° and 90°, while the set downstream contains eight kneading paddles at stagger angles of 60°. The die is comprised of a through hole of 3 mm diameter and 10 mm length. The barrel temperature was set at 200°C and the screw speed at 100 rpm. The G-HDPE, HDPE-g-MAH and HA dried powders were thoroughly mixed in the desired proportions (Table 1) and then introduced into the extruder at a feed rate of 1.5 kg h<sup>-1</sup> using a Brabender feeder. Extruded strands were cooled in a water bath immediately after passing through the die and then pelletized.

Specimens (type I tensile bars – ASTM D638) were injection-molded from the extruded pellets using an Arburg Allrounder 270V machine, under the following conditions: barrel temperature profile 200°C, 205°C, 210°C, 215°C and 220°C, mold temperature 40°C, flow rate 30 cm<sup>3</sup> s<sup>-1</sup>, holding pressure 250 bar for 7 s and mold cooling time 30 s.

### 2.5. Mechanical testing of the G-HDPE/HA/HDPE-g-MAH composites

Tensile testing was carried-out according to ASTM D638 on injection molded type I specimens in an Instron 5569 system at a crosshead speed of 50 mm min<sup>-1</sup>. Flexural testing (3-point bending) was carried-out according to ASTM D790 on standard bars machined from injection molded specimens using an Instron 5569 system at a crosshead speed of 1.27 mm min<sup>-1</sup>. Notched Izod impact strength testing was carried-out according to ASTM D256 on standard bars machined from injection molded specimens using a CEAST Resil 25 pendulum-type impact tester with 2.75 J energy capacity.

Each mechanical test value was calculated from the average value of five independent measurements. The standard deviations of each value were calculated and are shown as error bars in Tables.

### 2.6. Thermal analysis of the G-HDPE/HA/HDPE-g-MAH composites

The thermal studies were performed in a differential scanning calorimetry (DSC) system (PerkinElmer, DSC 6000). The G-HDPE, G-HDPE/HA and all composite formulations (Table 1) were analyzed. The crystallization temperature (T<sub>c</sub>) was obtained from first cooling DSC curves and the melting temperature (T<sub>m</sub>) and melting enthalpy (ΔH<sub>m</sub>) were obtained from second heating DSC curves. The heating procedure was performed with temperature ranging from 30°C to 200°C with heating rate of 10°C/min; and the cooling was performed with temperature ranging from 200°C to 30°C with cooling rate of 5°C min<sup>-1</sup>. A single sample for each composite was analyzed. All experiments were carried out in a nitrogen atmosphere (20 mL min<sup>-1</sup>).

The degree of crystallinity (X<sub>c</sub>) of the polymer matrix in the composites were determined using Equation 1:

$$X_c = \frac{\Delta H_m}{\Delta H_m^{100\%} \cdot (1 - \phi)} \quad (1)$$

Where ΔH<sub>m</sub> is the melting enthalpy of the sample, ΔH<sub>m</sub><sup>100%</sup> is the melting enthalpy for 100% crystalline HDPE (290 J g<sup>-1</sup>)<sup>25</sup> and φ is the weight fraction of hydroxyapatite in the composite.

### 2.7. Microscopy characterization of the G-HDPE/HA/HDPE-g-MAH composites

The morphologies of the composites were assessed by scanning electron microscopy (SEM) using a FEI Inspect S50 instrument operated at an acceleration voltage of 10 kV and a magnification of 20000 times. Samples (notched Izod impact specimens) were fractured after immersion in liquid nitrogen and then sputter-coated with gold prior to SEM examination.

### 2.8. In-vitro biological tests of the G-HDPE/HA/HDPE-g-MAH composites

In vitro hydrolytic degradation tests were performed with all composite formulations (Table 1) to identify possible degradations caused by a phosphate-buffered saline solution (PBS), which simulates biological systems, according to the methodology proposed by Macuvele et al.<sup>4</sup>.

**Table 1.** Design of experiments approach used to structure the experiments and to define the studied formulations.

Sample	Compositions	G-HDPE (wt%) *	HA (wt%) *	HA codified content	HDPE-g-MAH (wt%) **	HDPE-g-MAH codified content
1	G-HDPE/HA_10/HDPE-g-MAH_10	89.00	10.00	-1	10.00	-1
2	G-HDPE/HA_30/HDPE-g-MAH_10	67.00	30.00	+1	10.00	-1
3	G-HDPE/HA_10/HDPE-g-MAH_30	87.00	10.00	-1	30.00	+1
4	G-HDPE/HA_30/HDPE-g-MAH_30	61.00	30.00	+1	30.00	+1
5	G-HDPE/HA_34.1/HDPE-g-MAH_20	59.08	34.10	+1.41	20.00	0
6	G-HDPE/HA_5.9/HDPE-g-MAH_20	92.92	5.90	-1.41	20.00	0
7	G-HDPE/HA_20/HDPE-g-MAH_34.1	73.18	20.00	0	34.10	+1.41
8	G-HDPE/HA_20/HDPE-g-MAH_5.9	78.82	20.00	0	5.90	-1.41
9	G-HDPE/HA_20/HDPE-g-MAH_20	76.00	20.00	0	20.00	0
10	G-HDPE/HA_20/HDPE-g-MAH_20	76.00	20.00	0	20.00	0
11	G-HDPE/HA_20/HDPE-g-MAH_20	76.00	20.00	0	20.00	0

\* Relative to the total weight of the composite. \*\* Relative to the weight of the hydroxyapatite (HA) in the composite.

The PBS solutions were prepared with NaCl (82.0 g L<sup>-1</sup>) and Na<sub>2</sub>HPO<sub>4</sub> (10.5 g L<sup>-1</sup>). Tests were carried out with cylinder shaped samples, with diameter 2.00 mm and height 3.00 mm, produced with all compositions showed in Table 1. The mass of each sample was measured with an analytical balance (SHIMADZU, ± 0.01 g) and three samples of each composition were placed in individual test tubes containing 5.00 mL of PBS and kept in an oven at 37°C, with ambient atmosphere. The mass of each sample was measured after 8, 15, 30, 45, 60 and 90 days of storage times in the oven. For these procedures, samples were removed from test tubes and stored in a vacuum desiccator for 24 hours and after the mass was measured. After these procedures, the samples were replaced in the test tubes and in the oven to continue the immersion time in the PBS solution.

The hydrolytic degradation percentage (HD%) was determined according to the methodology proposed by Macuvele et al.<sup>5</sup>, for all samples and for all immersion times in the oven, using Equation 2.

$$HD\% = \left( \frac{m - m_i}{m_i} \right) \cdot 100\% \quad (2)$$

Where  $m_i$  is the initial mass and  $m$  is the sample mass after the immersion in PBS solution and exposition in the oven.

Hemolysis tests were performed according to the methodology proposed by Macuvele et al.<sup>4</sup> for a composite containing high amounts of hydroxyapatite (30 wt%) and HDPE-g-MAH (30 wt% relative to HA content) to identify negative effects on the blood of humans. The tests were performed in triplicate according to the methodology proposed by Macuvele et al.<sup>4</sup>, with human blood collected from a healthy voluntary donor, and after approval of the procedures by the ethics committee (CAAE 2533611960000116). Samples were immersed in test tubes with 2.0 mL of PBS and incubated in an oven at 37°C for 48 hours. After this time, the PBS solution was replaced by a new PBS and blood solution, prepared with 1.5 mL of PBS and 225 µL of blood diluted 1.25 times in PBS (negative control). The positive control was prepared with 1.5 mL of distilled water and 225 µL of blood solution diluted 1.25 times in PBS<sup>5</sup>.

After the incubation time (3 h), the solutions were centrifuged at 2000 rpm for 15 minutes and analyzed in an optical spectrophotometer (BioSystems, BTS-310) at a wavelength of 540 nm to determine the hemoglobin concentration released in the solution during the period of incubation. Percentage of hemolysis (H%) were determined using Equation 3.

$$H\% = \frac{C - C_n}{C_n - C_p} \quad (3)$$

Where  $C$  is hemoglobin concentration in the sample,  $C_n$  is the hemoglobin concentration in the negative control and  $C_p$  is the hemoglobin concentration in the positive control.

The positive control was prepared with the same amount of blood diluted in 1.5 mL of water, while the negative control was prepared with the same amount of blood in 1.5 mL of PBS<sup>4</sup>.

### 3. Results and Discussion

#### 3.1. Hydroxyapatite characterization

Figure 1 shows the X-ray diffractions patterns obtained for the synthesized calcium phosphate powder. According to the *Powder Diffraction Standards* (JCPDS-9-432) the major X-ray diffractions peaks are associated with the Ca<sub>5</sub>(PO<sub>4</sub>)<sub>3</sub>(OH) phase, typical of the hydroxyapatite crystalline structure (HA)<sup>26-28</sup>. The presence of β-tricalcium phosphate was identified by the 2θ values in 37.4 and 31.1<sup>29</sup>. The HA phase has mean crystallite size of 26 nm, which was estimated using the Debye-Scherrer equation<sup>29</sup> by the highest intensity X-ray peak (211). This value is in accordance with the Castro et al.<sup>30</sup>, that obtained values between 20-40 nm for the hydroxyapatite crystal sizes. Based on Rietveld refinement method, the synthesized product was composed of Ca<sub>5</sub>(PO<sub>4</sub>)<sub>3</sub>(OH) (74.5%) and tricalcium β-phosphate (phase with 25.5%), with the crystalline structure of hydroxyapatite being a hexagonal system, with unit cell lattice parameters equal to a = 9.42 Å and c = 6.88 Å.

The chemical composition of the synthesized hydroxyapatite was assessed by X-ray fluorescence spectroscopy (XRF), showed in Table 2. The major compounds detected were calcium (50.14%) and phosphorus (47.87%), associated with the calcium phosphate structures of the hydroxyapatite, and the Ca/P molar ratio was 1.71. Aluminum, magnesium and silicon with lower concentrations were detected and considered as impurity, but with tolerate amounts. Thus, the synthesized hydroxyapatite can be considered to have good chemical purity.

The particle size distribution of the synthesized hydroxyapatite (HA) is shown in Figure 2. A bimodal particle size distribution is observed with a small fraction (≈ 6%) of particles in the range 0.04 – 0.4 µm and a large fraction (≈ 94%) of particles in the range 0.6 – 30 µm.

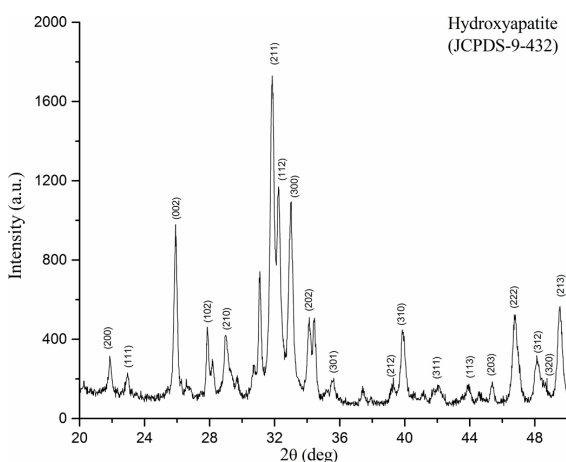


**Figure 1.** X-ray diffractogram obtained for the Hydroxyapatite (HA) - (JCPDS-9-432).

**Table 2.** Chemical composition of the synthesized hydroxyapatite performed by X-ray fluorescence spectroscopy (XRF).

Element	CaO	P <sub>2</sub> O <sub>5</sub>	MgO	SiO <sub>2</sub>	Al <sub>2</sub> O <sub>3</sub>	Fe <sub>2</sub> O <sub>3</sub>	K <sub>2</sub> O	MnO	Na <sub>2</sub> O	TiO <sub>2</sub>
(%)	50.14	47.87	0.59	0.50	0.10	<0.05	<0.05	<0.05	<0.05	<0.05

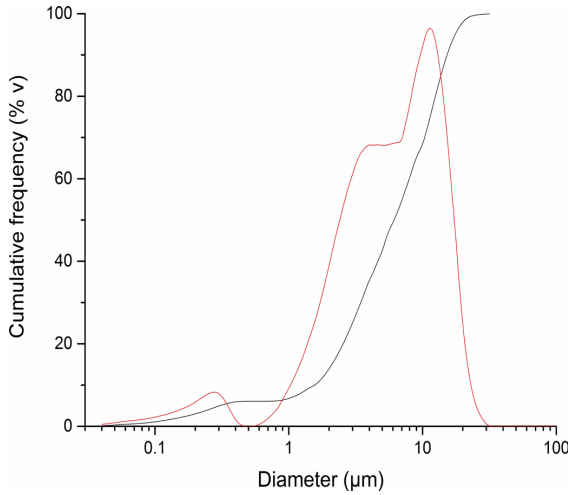


Figure 2. Particle size distribution curve for the Hydroxyapatite (HA).

The SEM images show uniform compact agglomerates of hydroxyapatite with primary particle size in the range 150-250 nm (Figure 3a and Figure 3b). The Figure 3c shows details in a particular region (R1) and reveals that the agglomerates are formed by organized nanostructures with dimensions of approximately 20-30 nm, in accordance with similar results reported by the scientific literature for agglomerates formed by HA nanoparticles with 20-100 nm<sup>29-32</sup> and with similar methods of precipitation and calcination synthesis<sup>33</sup>.

### 3.2. Mechanical properties of G-HDPE/HA/HDPE-g-MAH composites

Neat G-HDPE, G-HDPE/HA and G-HDPE/HA/HDPE-g-MAH composites with different compositions established by the design of experiments (Table 1) were characterized in terms of tensile, flexural and impact properties. Young modulus, yield stress, flexural modulus and notched Izod impact strength data are summarized in Table 3.

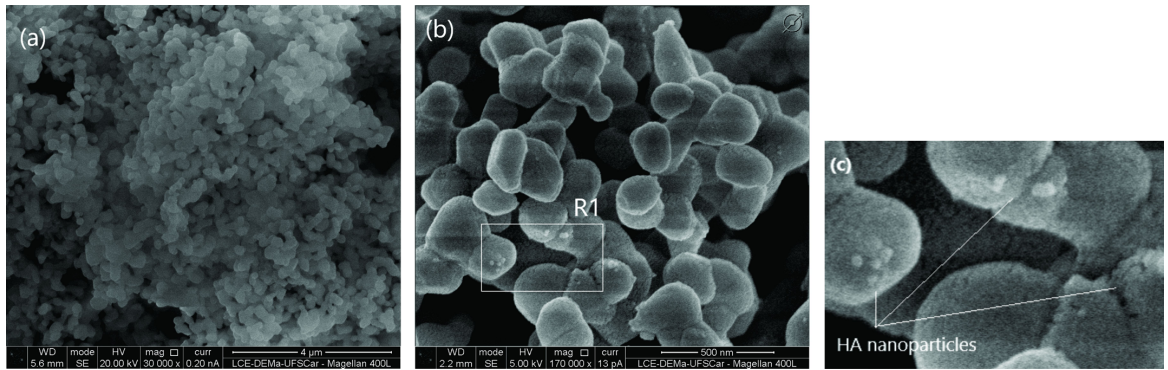


Figure 3. SEM images obtained for the hydroxyapatite (HA): (a) 30.000 times magnification, (b) 170.000 times magnification and (c) details of the compact HA agglomerates (R1).

Table 3. Mechanical properties determined for G-HDPE and G-HDPE/HA/HDPE-g-MAH composites with different compositions established by the design of experiments (Table 1).

Samples	Young modulus (GPa)	Yield Stress (MPa)	Flexural modulus (GPa)	Impact Strength (J/m)
G-HDPE	1.16 ± 0.01	20.48 ± 0.37	1.10 ± 0.03	164.5 ± 4.6
G-HDPE/HA 90/10	1.30 ± 0.04	20.88 ± 0.14	1.08 ± 0.05	75.8 ± 1.5
G-HDPE/HA 80/20	1.49 ± 0.17	20.77 ± 0.21	1.21 ± 0.01	112.2 ± 4.2
G-HDPE/HA 70/30	1.78 ± 0.09	20.48 ± 0.41	1.26 ± 0.07	76.1 ± 3.6
G-HDPE/HA_10/HDPE-g-MAH_10	1.39 ± 0.02	21.14 ± 0.10	0.96 ± 0.03	58.4 ± 1.9
G-HDPE/HA_30/HDPE-g-MAH_10	1.75 ± 0.04	23.36 ± 0.77	1.25 ± 0.10	40.1 ± 1.4
G-HDPE/HA_10/HDPE-g-MAH_30	1.36 ± 0.03	22.01 ± 0.32	0.96 ± 0.11	74.8 ± 1.4
G-HDPE/HA_30/HDPE-g-MAH_30	1.74 ± 0.03	25.27 ± 0.24	1.27 ± 0.07	53.0 ± 2.9
G-HDPE/HA_34.1/HDPE-g-MAH_20	1.88 ± 0.06	25.55 ± 0.19	1.38 ± 0.06	44.8 ± 2.8
G-HDPE/HA_5.9/HDPE-g-MAH_20	1.31 ± 0.02	21.64 ± 0.17	0.90 ± 0.05	66.3 ± 1.1
G-HDPE/HA_20/HDPE-g-MAH_34.1	1.64 ± 0.02	23.89 ± 0.21	1.16 ± 0.07	64.5 ± 2.4
G-HDPE/HA_20/HDPE-g-MAH_5.9	1.55 ± 0.03	22.56 ± 0.24	1.18 ± 0.08	43.2 ± 0.8
G-HDPE/HA_20/HDPE-g-MAH_20	1.62 ± 0.02	23.67 ± 0.11	1.15 ± 0.02	52.8 ± 1.7
G-HDPE/HA_20/HDPE-g-MAH_20	1.61 ± 0.03	23.09 ± 0.09	1.12 ± 0.05	53.1 ± 2.2
G-HDPE/HA_20/HDPE-g-MAH_20	1.59 ± 0.01	23.26 ± 0.19	1.19 ± 0.10	53.1 ± 1.3

Young modulus values of composites are higher than the value determined for the neat G-HDPE for all contents of hydroxyapatite (HA) and compatibilizer (HDPE-g-MAH) used, with the highest values being obtained for the composites produced with the highest HA content (Figure 4). While the Young modulus of neat G-HDPE is 1.16 GPa, the composite with 34.1 wt% of hydroxyapatite showed a value of 1.88 GPa, which represents an increase of 62%. The increase in the Young modulus is associated with the increase in the stiffness of the polymer matrix, thus suggesting that the deformation of the G-HDPE matrix is restricted by the presence of hydroxyapatite. Statistical analyses (ANOVA with  $p < 0.05$ ; Tukey test) revealed that the HDPE-g-MAH content is not significant and only the HA content has a significant effect on the Young modulus, with a linear relationship and with a good correlation coefficient of 0.95 (Equation 4).

$$E = 1.580(0.007) + 0.190(0.008) \cdot \text{HA}\% \quad (4)$$

where E is the Young modulus and HA% is the codified hydroxyapatite content (Table 1) in the composite.

The reinforcement level for the composites under study is expected to be small, since the hydroxyapatite used in this work has a small aspect ratio (HA particles are spherical). Notwithstanding, the Young modulus values for the composites under study are comparable to those reported in other studies for a given hydroxyapatite content<sup>1,7</sup>.

Yield stress values of composites increased with the increase in the hydroxyapatite (HA) and HDPE-g-MAH contents (Figure 5). Statistical analyses (ANOVA with  $p < 0.05$ ; Tukey test) revealed that hydroxyapatite and HDPE-g-MAH contents affect the yield stress, with a quadratic relation and with a good correlation coefficient of 0.92 (Equation 5).

$$\text{YS} = 23.35(0.07) + 1.38(0.06) \cdot \text{HA}\% + 0.58(0.06) \cdot \text{MAH}\% - 0.18(0.07) \cdot \text{MAH}\%^2 + 0.26(0.09) \cdot \text{HA}\% \cdot \text{MAH}\% \quad (5)$$

where YS is the yield stress, HA% is the codified hydroxyapatite content and MAH% is the codified HDPE-g-MAH content (Table 1) in the composite.

In the statistical model (Equation 5), linear terms have a greater contribution to yield stress values and are positive for the effects of the HA and HDPE-g-MAH. Furthermore, the positive interaction effect between the HA and HDPE-g-MAH contents suggests a synergistic effect between these two components. High density polyethylene is a nonpolar polymer, so the hydroxyapatite (polar) is mechanically anchored in the G-HDPE matrix. The anchoring process occurs with the retraction of the polymeric chains surrounding the HA clusters during the processing cooling step. On the other hand, the addition of the HDPE-g-MAH in the composite is expected to improve the dispersion and increase the adhesion of the hydroxyapatite particles in the G-HDPE matrix, leading to the increase in the yield stress values. In a study dedicated to polyolefin/hydroxyapatite composites, Albano et al.<sup>21</sup> showed that when HDPE is functionalized with maleic anhydride, the dispersion and distribution of hydroxyapatite particles is favored and the yield stress increases slightly.

Flexural modulus values of composites increased with the increase in the hydroxyapatite (HA) content (Figure 6).

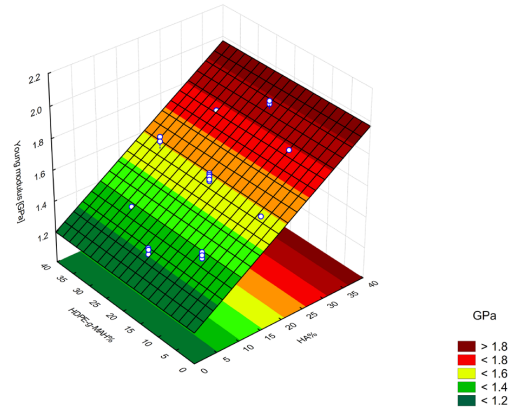


**Figure 4.** Response surface obtained from Equation 4 for Young modulus values and statistically significant variable (HA%).

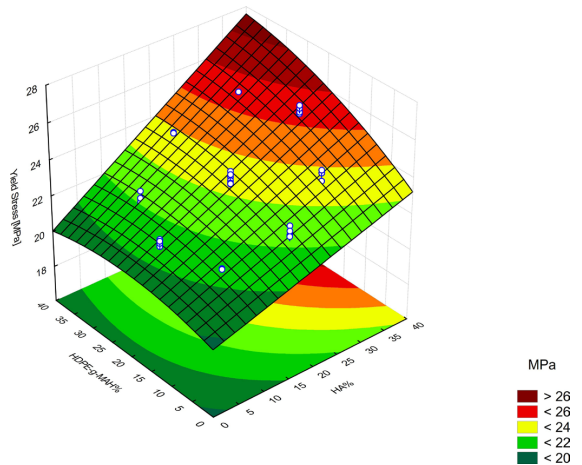


**Figure 5.** Response surface obtained from Equation 5 for yield stress values and statistically significant variables (HA% and MAH%).

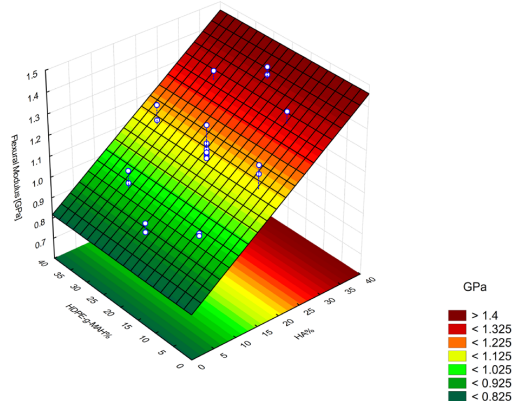


**Figure 6.** Response surface obtained from Equation 6 for flexural modulus values and statistically significant variable (HA%).

With concentrations of 30 wt% and 34.1 wt% of hydroxyapatite, composites showed a flexural modulus above 1.25 MPa, an increase of 12% over neat G-HDPE, which has a flexural modulus value of 1.10 MPa. Similar to the results obtained with the tensile tests, statistical analyses (ANOVA with  $p < 0.05$ ; Tukey test) reveals that the HDPE-g-MAH content is not significant and only the hydroxyapatite content affects the values of flexural modulus, with a linear relationship and a reasonable correlation coefficient of 0.81 (Equation 6).

$$EF = 1.14(0.01) + 0.16(0.01) \cdot HA\% \quad (6)$$

where EF is the flexural modulus and HA% is the codified hydroxyapatite content (Table 1) in the composite.

Notched Izod impact strength values of composites are affected by the HA and HDPE-g-MAH contents (Figure 7). The increase in the HA content causes a significant decrease in the impact strength to values between 40 J/m and 70 J/m, while neat G-HDPE shows an impact strength of 164 J/m. Differently, the addition of the HDPE-g-MAH increases the impact strength even with a high hydroxyapatite content in the composite. For the composite with 30 wt% of hydroxyapatite, the increase in the HDPE-g-MAH content from 10 wt% to 30 wt% increased the impact strength from 40 J/m to 53 J/m, which represents an increase of 13%. Statistical analyses (ANOVA with  $p < 0.05$ ; Tukey test) revealed that the hydroxyapatite and HDPE-g-MAH contents affect the impact strength values with a quadratic relation and with a good correlation coefficient of 0.95 (Equation 7).

$$IS = 52.97(0.60) - 8.83(0.37) \cdot HA\% + 7.44(0.37) \cdot MAH\% - 1.77(0.44) \cdot HA\%^2 + 0.90(0.44) \cdot MAH\%^2 \quad (7)$$

where IS is the notched Izod impact strength, HA% is the codified hydroxyapatite content and MAH% is the codified HDPE-g-MAH content (Table 1) in the composite.

The decrease in the impact strength of composites with addition of hydroxyapatite is in agreement with the study reported by Zhang and Tanner<sup>6</sup>, which showed a reduction in the impact strength of HDPE based composites with increasing amounts of hydroxyapatite. The authors attributed this to the weak interactions between the hydroxyapatite agglomerates and the polymer matrix, which results in the formation of voids (organizational failures) and, consequently, in the formation of cracks and their propagation during the impact test. On the other hand, the addition of the HDPE-g-MAH in the composites is expected to improve the dispersion and increase the adhesion of the hydroxyapatite phase in the G-HDPE matrix, leading to the increase in the impact strength values.

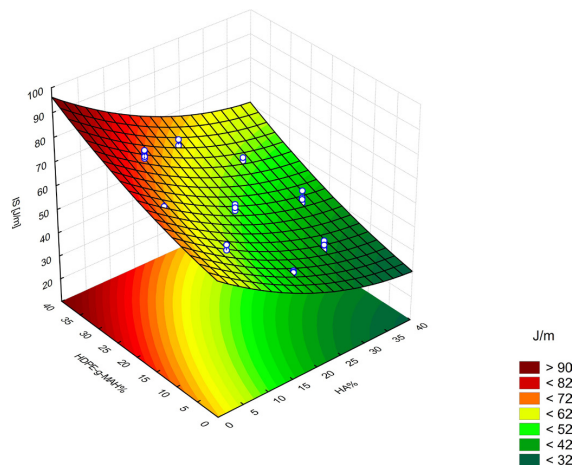
### 3.3. Morphology of G-HDPE/HA/HDPE-g-MAH composites

Figure 8a-d shows SEM images of cryo-fractured surfaces of some selected composites. In the composites without HDPE-g-MAH, the hydroxyapatite appears as clusters with sizes between 500 nanometers and 2 micrometers, which are distributed throughout the G-HDPE matrix. When the hydroxyapatite content is increased, the size of the clusters does not change significantly, but the number of clusters per volume is higher (Figure 8a-b).

The interface with the G-HDPE matrix is weak, as indicated by the voids shown in the region 1 of the Figure 8b. The addition of HDPE-g-MAH in the composites significantly change the distribution and size of the hydroxyapatite clusters throughout the G-HDPE matrix. With the addition of 10 wt% HDPE-g-MAH, hydroxyapatite clusters with more uniform dimensions are formed throughout the polymer matrix (Figure 8c). When the HDPE-g-MAH content is increased to 30 wt%, the clusters are less compact and smaller (Figure 8d), which indicates a better dispersion of hydroxyapatite particles in G-HDPE. The reduction in the dimensions of the hydroxyapatite clusters and the absence of voids at the interface between the agglomerates and the polymer matrix are noticeable.

Thus, it is possible to infer that maleic anhydride grafted high density polyethylene (HDPE-g-MAH) acts as a compatibilizing agent for the composites of G-HDPE and hydroxyapatite (HA) developed in this study. This is in agreement with the studies performed by Albano et al.<sup>21</sup> and Balakrishnan et al.<sup>22</sup> who suggested that maleic anhydride unit can interact chemically with hydroxyapatite polar groups. This produces a strong polymer/particle interface that helps to disperse and distribute the particles in the polymer matrix during melting processing<sup>34</sup>.

As shown in the previous section, the effects of addition of HDPE-g-MAH are statistically relevant only for the non-elastic properties of the composites, namely, yield stress (Figure 5; Equation 5) and impact strength (Figure 7; Equation 7). This is because these properties are highly dependent on interfacial adhesion, as well as the degree of dispersion that dictates the interfacial area. So, as HDPE-g-MAH improved the dispersion and adhesion of hydroxyapatite in the G-HDPE matrix (Figure 8a-d), yield stress and impact strength values for the composites were increased with the increase in the HDPE-g-MAH content relative to the HA phase. In a different way, tensile (Young) and flexural modulus, being quasi-elastic properties, are not influenced by interfacial adhesion, although they are dependent on interfacial area. So, the addition of HDPE-g-MAH did not affect these properties, which were influenced only by the hydroxyapatite (HA) content (Figures 4 and 6; Equations 4 and 6).



**Figure 7.** Response surface obtained from Equation 7 for impact strength values and statistically significant variables (HA% and MAH%).

### 3.4. Thermal characterization

Differential scanning calorimetry (DSC) was used to investigate the melting and crystallization of the polymer matrix in the G-HDPE/HA/HDPE-g-MAH composites.

Figures 9a and 9b show, respectively, the thermal responses obtained in the cooling and in the second heating

for some selected composites. From the DSC curves the values of the melting temperature ( $T_m$ ), crystallization temperature ( $T_c$ ) and the respectively melting enthalpy ( $\Delta H_m$ ) were determined. The degree of crystallinity ( $X_c$ ) was determined using the Equation 1. These values are shown in Table 4.

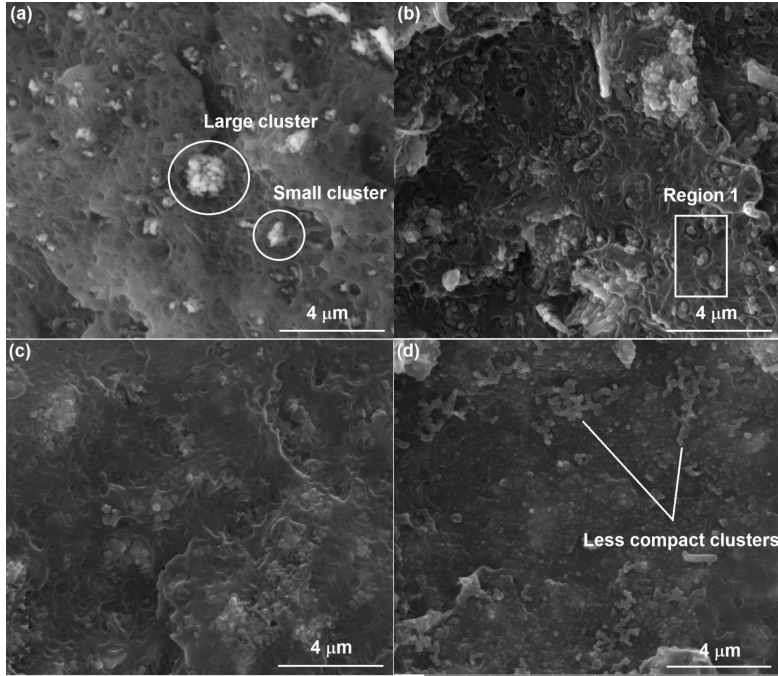


**Figure 8.** SEM images of some selected G-HDPE/HA and G-HDPE/HA/HDPE-g-MAH composites. (a) G-HDPE with 10 wt% HA, (b) G-HDPE with 30 wt% HA, (c) G-HDPE with 30 wt% HA and 10 wt% HDPE-g-MAH, (d) G-HDPE with 30 wt% HA and 30 wt% HDPE-g-MAH.

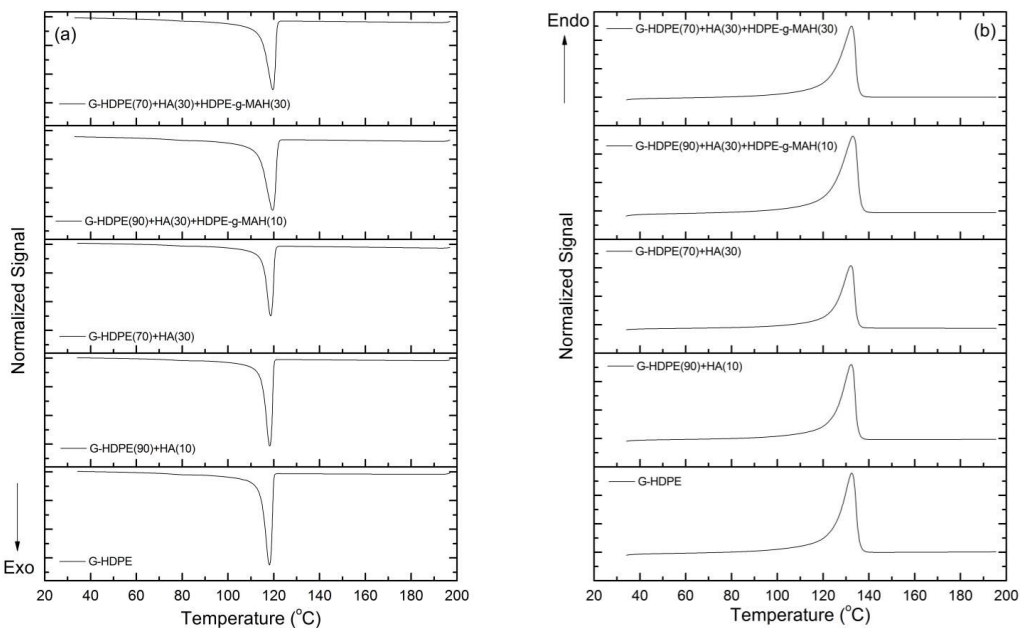


**Figure 9.** DSC curves obtained in the (a) first cooling and (b) second heating of the composites: G-HDPE, G-HDPE/HA 90/10, G-HDPE/HA 70/30, G-HDPE with 30 wt% HA and 10 wt% HDPE-g-MAH and G-HDPE with 30 wt% HA and 30 wt% HDPE-g-MAH.

**Table 4.** Crystallization temperatures ( $T_c$ ), melting temperatures ( $T_m$ ) and respective melting enthalpy ( $\Delta H_m$ ), determined from DSC for G-HDPE, G-HDPE/HA and G-HDPE/HA/HDPE-g-MAH composites with different compositions established by the design of experiments (Table 1). Degree of crystallinity ( $X_c$ ) determined using the Equation 1.

Composition	$T_c$ (°C)	$T_m$ (°C)	$\Delta H_m$ (J/g)	$X_c$ (%)
G-HDPE	118.0	133.0	180	62
G-HDPE/HA 90/10	118.0	132.0	172	66
G-HDPE/HA 80/20	119.0	131.0	188	81
G-HDPE/HA 70/30	119.0	132.0	141	70
G-HDPE/HA_10/HDPE-g-MAH_10	119.0	133.0	137	52
G-HDPE/HA_30/HDPE-g-MAH_10	120.0	133.0	121	59
G-HDPE/HA_10/HDPE-g-MAH_30	119.0	134.0	109	42
G-HDPE/HA_30/HDPE-g-MAH_30	120.0	132.0	133	65
G-HDPE/HA_34.1/HDPE-g-MAH_20	120.0	133.0	114	59
G-HDPE/HA_5.9/HDPE-g-MAH_20	119.0	133.0	119	44
G-HDPE/HA_20/HDPE-g-MAH_34.1	120.0	132.0	144	62
G-HDPE/HA_20/HDPE-g-MAH_5.9	120.0	132.0	153	66
G-HDPE/HA_20/HDPE-g-MAH_20	120.0	133.0	131	57
G-HDPE/HA_20/HDPE-g-MAH_20	120.0	132.0	127	55
G-HDPE/HA_20/HDPE-g-MAH_20	120.0	132.0	142	61

The DSC curves showed only one melting transition and only one crystallization transition for all compositions studied, indicating the addition of hydroxyapatite and HDPE-g-MAH does not induce new crystallization phases in the G-HDPE matrix polymer. Statistical analyses (ANOVA with  $p < 0.05$ ; Tukey test) showed that melting temperature ( $T_m$ ) values were not significantly changed with the addition of hydroxyapatite and HDPE-g-MAH. Differently, the hydroxyapatite content influences the crystallization temperature ( $T_c$ ) values, while the HDPE-g-MAH does not have influence on this property. The surface responses for the crystallization temperature ( $T_c$ ) and the degree of crystallinity ( $X_c$ ) of the polymer matrix in the composites are shown in Figure 10a-b.

The effect of the hydroxyapatite content in the crystallization temperature follows a quadratic relation, with a good correlation coefficient of 0.91 (Equation 8).

$$T_c = 119.94(0.06) + 0.43(0.05).HA\% - 0.30(0.06).HA\%^2 \quad (8)$$

Where  $T_c$  is crystallization temperature of the polymer matrix and HA% is the codified hydroxyapatite content (Table 1) in the composite.

The statistical analysis revealed that the degree of crystallinity is influenced only by the hydroxyapatite content, with no significant influence of the HDPE-g-MAH content. A quadratic model was established between the degree of crystallinity and the hydroxyapatite content in the composite, with a good correlation coefficient of 0.85 (Equation 9).

$$X_c = 59.87(1.95) + 6.65(1.64).HA\% - 4.51(1.87).HA\%^2 \quad (9)$$

Where  $X_c$  is the degree of crystallinity of the polymer matrix and HA% is the codified hydroxyapatite content (Table 1) in the composite.

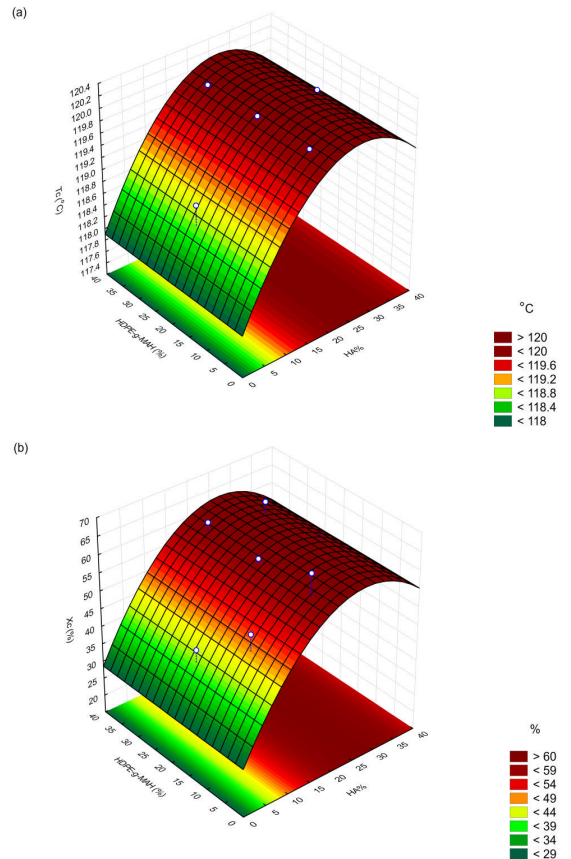


**Figure 10.** Response surface obtained from Equation 8 and Equation 9. (a) Composite crystallization temperature ( $T_c$ ) values and statistically significant variable (HA%) and (b) Degree of crystallinity ( $X_c$ ) values and statistically significant variable (HA%).

According to the statistical model, the maximum crystallization temperature value is 120.7 °C, which corresponds to a 2.3% increase in the crystallization temperature as compared to the neat G-HDPE (118.0 °C). The increase in the  $T_c$  suggests that hydroxyapatite act as a heterogeneous nucleating agent for the G-HDPE matrix, which corroborates the study by Li and Tjong<sup>7</sup>. The increase in the hydroxyapatite content up to 32 wt% increases the degree of crystallinity of the polymer matrix, but the effect is negative for higher amounts (Figure 10a). According to the statistical model, the maximum value of the crystallization degree is 73%, which corresponds to a 17% increase in the crystallization degree as compared to the neat G-HDPE (Figure 10b). Elastic modulus and yield stress values of HDPE are expected to increase with the degree of crystallinity. Nevertheless, the individual effect of the degree of crystallinity on these properties was not evaluated in the manuscript, but the indirect effect due to the different hydroxyapatite contents in the composites were accounted for.

### 3.5. In vitro degradation with PBS

Hydrolytic degradation tests were performed for all composite samples (Table 1) and the percentage value of mass loss of the samples after immersion in the simulated solution was determined, with a negative value indicating a positive effect of hydrolytic degradation. In general, there was no significant loss of mass (HD% is nearly zero) with time during the hydrolytic degradation test of the samples, indicating that HA and HDPE-g-MAH do not affect the hydrolytic stability of the G-HDPE matrix in the simulated solutions. On the other hand, the composites with hydroxyapatite contents greater than 20 wt% showed an increase in the mass after 90 days of immersion. For the composite containing 30 wt% hydroxyapatite the increase of the mass was of 8%, while the mass for the neat G-HDPE sample without HA showed no significant variation (Figure 11). The increase in mass may be associated with the formation of sodium crystals or calcium phosphate that may originate from the phosphate ions of the PBS solution with calcium ions present in the composite. In any case, this hypothesis should be evaluated in a future study.

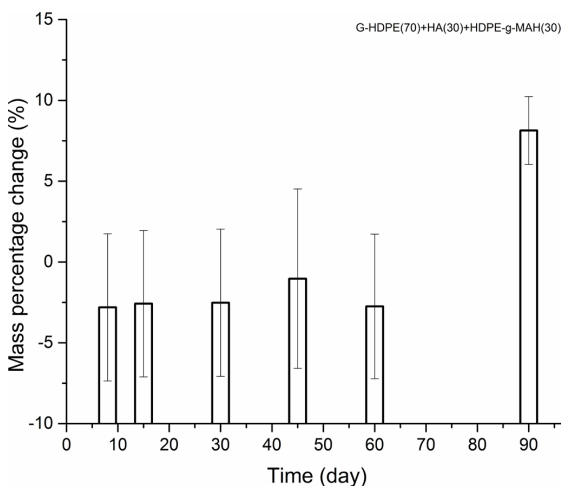
### 3.6. Hemocompatibility

Table 5 shows the hemolysis results obtained for the composite containing 30 wt% of HA and 30 wt% (relative to the HA content) of HDPE-g-MAH. The values of the percentage of hemolysis (%H) are negative for the composite and can be consider null, according to the standard ISO 10993.

**Table 5.** Hemolysis results obtained for the G-HDPE with 30 wt% of hydroxyapatite and 30 wt% of HDPE-g-MAH. Solution of blood diluted in PBS and the absorbances values measured in 540 nm wavelength of the absorbance spectrums. Percentage of Hemolysis (%H) determined by Equation 3.

Sample	Absorbance (540 nm)	%H
Positive Control	0.3238	100.0
Negative Control	0.0822	0.0
G-HDPE + HA (30) + HDPE-g-MAH (30) – sample 1	0.0759	-2.6
G-HDPE + HA (30) + HDPE-g-MAH (30) – sample 2	0.0755	-2.8
G-HDPE + HA (30) + HDPE-g-MAH (30) – sample 3	0.0731	-3.8

Figure 12 shows a graphical comparative between the percentage of hemolysis for the positive control, negative control and for this composite. This test suggests this composite is a promising material to be used in bone tissue engineering.



**Figure 11.** Hydrolytic degradation results for the G-HDPE with 34.1 wt% HA and 20 wt% HDPE-g-MAH after immersion in simulated solution (PBS) by different times.

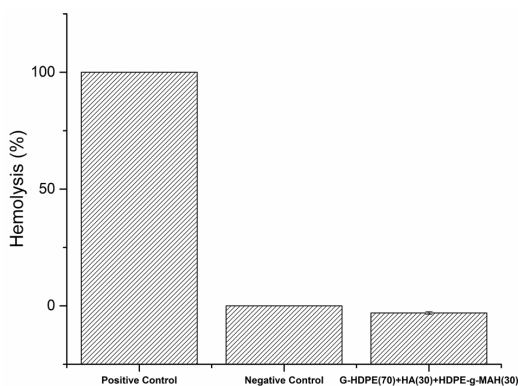


**Figure 12.** Graphical comparative between of percentage of hemolysis for the positive control, negative control and for the G-HDPE with 30 wt% HA and 30 wt% HDPE-g-MAH.

## 4. Conclusions

Composites based on green high-density polyethylene (G-HDPE) filled with hydroxyapatite particles (HA) compatibilized with maleic anhydride grafted polyethylene (HDPE-g-MAH) were developed through a design of experiments approach. The optimized mechanical, thermal and biocompatibility properties suggest the composite is a promising material for bone tissue engineering, for application in bone implants and grafts.

The interface between the hydroxyapatite phase and the G-HDPE matrix was improved with the addition of HDPE-g-MAH, which acts as a compatibilizing agent, reducing the size of hydroxyapatite clusters and improving the distribution in the polymer matrix.

The addition of hydroxyapatite and HDPE-g-MAH did not induce new crystalline phases in G-HDPE and the melting temperature values were not significantly changed, but the hydroxyapatite content had a positive quadratic effect on the crystallization temperature and the degree of crystallinity of the polymer matrix, with no significant influence of the HDPE-g-MAH content.

The stiffness and strength of composites can be modulated and optimized by the composition. Increasing the HA content leads to an increase in the modulus and yield strength and a decrease in impact strength, while the increase in the HDPE-g-MAH content increases the yield and impact strengths, with negligible influence on the modulus of the composites. In general, the composite containing 30 wt% HA (relative to the total weight of the composite) and 30 wt% HDPE-g-MAH (relative to the weight of HA in the composite) showed a better balance of mechanical properties.

Hemolysis test performed on the composite with best mechanical performance did not indicate significant hydrolytic degradation.

## 5. Acknowledgments

This work was supported by CNPq – National Council for Scientific and Technological Development, Brazil (grant numbers 309258/2020-0 and 310076/2020-0), CAPES – Coordenação de Aperfeiçoamento de Pessoal de Nível Superior, Brazil (grant number 23038.021524.2016.88). This study was financed in part by the Coordenação de Aperfeiçoamento de Pessoal de Nível Superior - Brasil (CAPES) - Finance Code 001. The authors are grateful to the Laboratory of Structural Characterization (LCE/DEMa/UFSCar) for use of the general facilities.

## 6. References

- Bonfield W. Hydroxyapatite-reinforced polyethylene as an analogous material for bone replacement. *Ann N Y Acad Sci.* 1988;523:173-7.
- Liu T, Huang K, Li L, Gu Z, Liu X, Peng X, et al. High performance high-density polyethylene/hydroxyapatite nanocomposites for load-bearing bone substitute: fabrication, in vitro and in vivo biocompatibility evaluation. *Compos Sci Technol.* 2019;175:100.
- Kribaa OK, Latif S, Saifi F, Chahbaoui N. Elaboration and chemical characterization of a composite material based on hydroxyapatite / polyethylene. *Mater Today Proc.* 2022;49(4):1017-22.
- Macuvele DLP, Colla G, Cesca K, Ribeiro LFB, Costa CE, Nones J, et al. UHMWPE/HA biocomposite compatibilized by organophilic montmorillonite: an evaluation of the mechanical-tribological properties and its hemocompatibility and performance in simulated blood fluid. *Mater Sci Eng C.* 2019;100:411-23.
- Macuvele DLP, Nones J, Matsinhe JV, Lima MM, Soares C, Fiori MA, et al. Advances in ultra-high molecular weight polyethylene/hydroxyapatite composites for biomedical applications: a brief review. *Mater Sci Eng C.* 2017;76:1248-62.
- Zhang Y, Tanner KE. Impact behavior of hydroxyapatite reinforced polyethylene composites. *J Mater Sci Mater Med.* 2003;14:63-8.
- Li K, Tjong SC. Preparation and mechanical and tribological properties of high-density polyethylene/hydroxyapatite nanocomposites. *J Macromol Sci Part B Phys.* 2011;50(7):1325-37.
- Lett A, Sagadevan S, Fatimah I, Hoque ME, Lokanathan Y, Léonard E, et al. Recent advances in natural polymer-based hydroxyapatite scaffolds: properties and applications. *Eur Polym J.* 2021;148:110360.
- Sindhya A, Jeyakumar SJ, Jothibas M, Pugalendhi P. Synthesis and characterization of nanohydroxyapatite (nHAp) from Meretrix Meretrix Clam shells and its in-vitro studies for biomedical applications. *Vacuum.* 2022;204:111341.
- Abere DV, Ojo SO, Oyatogun GM, Paredes-Epinosa MB, Niluxshun MCD, Hakami A. Mechanical and morphological characterization of nano-hydroxyapatite (nHA) for bone regeneration: a mini review. *Biomedical Engineering Advances.* 2022;4:100056.
- Belboom S, Léonard A. Does biobased polymer achieve better environmental impacts than fossil polymer? Comparison of fossil HDPE and biobased HDPE produced from sugar beet and wheat. *Biomass Bioenergy.* 2016;85:159-67.
- Dorozhkin SV. Calcium orthophosphate deposits: preparation, properties and biomedical applications. *Mater Sci Eng C.* 2015;55:272-326.
- Gervaso F, Scalera F, Padmanabhan K, Sannino S, Licciulli A. High-performance hydroxyapatite scaffolds for bone tissue engineering applications. *Int J Appl Ceram Technol.* 2012;9:507-16.
- Sousa AF, Silvestre AJD. Plastics from renewable sources as green and sustainable alternatives. *Curr Opin Green Sustain Chem.* 2022;33:100557.
- Zhang Y, Duan C, Bokka SK, He Z, Ni Y. Molded fiber and pulp products as green and sustainable alternatives to plastics: A mini review. *Journal of Bioresources and Bioproducts.* 2022;7(1):14-25.
- Mehrabani SAN, Vatanpour V, Koyuncu I. Green solvents in polymeric membrane fabrication: a review. *Separ Purif Tech.* 2022;298:121691.
- Komaki Y, Tsukamoto T, Oishi Y, Shibasaki Y. Green polymer synthesis and low dielectric properties obtained by oxidative polymerization of thymol with CuCl<sub>2</sub>-(p-tolyl)pyridine catalyst. *React Funct Polym.* 2022;172:105206.
- Mazur K, Jakubowska P, Romańska P, Kuciel S. Green high density polyethylene (HDPE) reinforced with basalt fiber and agricultural fillers for technical applications. *Compos, Part B Eng.* 2020;202:108399.
- Jermolovicius LA, Ponzada EVS, Nascimento RB, Castro ER, Senise JT, Mente BB, Martins MC, et al. Greening the green ethylene with microwaves. *Chem Eng Process.* 2018;127:238-48.
- Tarrés Q, Melbø JK, Delgado-Aguilar M, Espinach FX, Mutjé P, Chinga-Carrasco G. Bio-polyethylene reinforced with thermomechanical pulp fibers: mechanical and micromechanical characterization and its application in 3D-printing by fused deposition modelling. *Compos, Part B Eng.* 2018;153:70-7.
- Albano C, Perera R, Cataño L, Alvarez S, Karam A, González G. Compatibilization of polyolefin/hydroxyapatite composites using grafted polymers. *Polym Plast Technol Eng.* 2010;49(4):341-6.

22. Balakrishnan H, Husin MR, Wahit MU, Kadir MRA. Maleated high density polyethylene compatibilized high density polyethylene/hydroxyapatite composites for biomedical applications: properties and characterization. *Polymer-Plastics Technology and Materials*. 2013;52(8):774-82.
23. Hao X, Xu J, Zhou H, Tang W, Li L, Wang Q, et al. Interfacial adhesion mechanisms of ultra-highly filled wood fiber/polyethylene composites using maleic anhydride grafted polyethylene as a compatibilizer. *Mater Des*. 2021;212:110182.
24. Chang MK. Mechanical properties and thermal stability of low-density polyethylene grafted maleic anhydride/montmorillonite nanocomposites. *J Ind Eng Chem*. 2015;27:96-101.
25. Canevarolo SV. *Ciência dos polímeros*. São Paulo: Ed. Artliber; 2006.
26. Martinez C, Gattina GL, Garrido L, Gilabert U, Ozols A. Hydroxyapatite microsphere production by plasma spray. *Procedia Materials Science*. 2015;8:319-23.
27. Han JK, Song HY, Saito F, Lee BT. Synthesis of high purity nano-sized hydroxyapatite powder by microwave-hydrothermal method. *Mater Chem Phys*. 2006;99:235-9.
28. Hsieh MF, Perng LH, Chin TS, Perng HG. Phase purity of sol-gel-derived hydroxyapatite ceramic. *Biomaterials*. 2001;22(19):2601-7.
29. Corrêa THA, Holanda JNF. Fish bone as a source of raw material for synthesis of calcium phosphate. *Mater Res*. 2019;22(1):e20190486.
30. Castro MAM, Portela TO, Correa GS, Oliveira MM, Rangel JHG, Rodrigues SF, et al. Synthesis of hydroxyapatite by hydrothermal and microwave irradiation methods from biogenic calcium source varying pH and synthesis time. *Bol Soc Esp Ceram Vidr*. 2022;61(1):35-41.
31. Pietrasik J, Szustakiewicz K, Zaborski M, Haberko K. Hydroxyapatite: an environmentally friendly filler for elastomers. *Mol Cryst Liq Cryst (Phila Pa)*. 2008;483:172-8.
32. Shahgholi M, Karimipour A, Firouzi P, Malekhamdi O, Ghashang M, Saadoon N, et al. Fabrication and characterization of synthesized hydroxyapatite/ethanolamine for bone tissue engineering application. *Colloids Surf A Physicochem Eng Asp*. 2022;650:129591.
33. Sebastiammal S, Fathima ASL, Alarifi A, Henry SMJ, Kavipriya MR, Govindarajan M, et al. Synthesis and physicochemical characteristics of Ag-doped hydroxyapatite nanoparticles, and their potential biomedical applications. *Environ Res*. 2022;210:112979.
34. Sharifzadeh E, Maleki M. An energy-based approach to study the aggregation/agglomeration phenomenon in polymer nanocomposites: dispersion force against inter-particle cohesion. *Polym Compos*. 2022;43:5145-58.